

# Comparison of GMF/GPT with VMF1/ECMWF and implications for atmospheric loading

Peter Steigenberger · Johannes Boehm ·  
Volker Tesmer

Received: 27 August 2008 / Accepted: 3 March 2009 / Published online: 26 March 2009  
© Springer-Verlag 2009

**Abstract** This paper compares estimates of station coordinates from global GPS solutions obtained by applying different troposphere models: the Global Mapping Function (GMF) and the Vienna Mapping Function 1 (VMF1) as well as a priori hydrostatic zenith delays derived from the Global Pressure and Temperature (GPT) model and from the European Centre for Medium-Range Weather Forecasts (ECMWF) numerical weather model data. The station height differences between terrestrial reference frames computed with GMF/GPT and with VMF1/ECMWF are in general below 1 mm, and the horizontal differences are even smaller. The differences of annual amplitudes in the station height can also reach up to 1 mm. Modeling hydrostatic zenith delays with mean (or slowly varying empirical) pressure values instead of the true pressure values results in a partial compensation of atmospheric loading. Therefore, station height time series based on the simple GPT model have a better repeatability than those based on more realistic ECMWF troposphere a priori delays if atmospheric loading correc-

tions are not included. On the other hand, a priori delays from numerical weather models are essential to reveal the full atmospheric loading signal.

**Keywords** Troposphere modeling · Mapping function · Atmospheric loading · GPS

## 1 Introduction

Due to the correlations between the troposphere zenith delays and the station heights (e.g., Rothacher 2002), a sophisticated modeling of the troposphere is a prerequisite for the estimation of precise coordinates from space geodetic microwave techniques, namely Global Navigation Satellite Systems (GNSS) like the Global Positioning System (GPS), Very Long Baseline Interferometry (VLBI), and Doppler Orbitography and Radiopositioning Integrated by Satellite (DORIS). Troposphere parameters estimated by different techniques have been compared by, e.g., Snajdrova et al. (2005) and Steigenberger et al. (2007). The tropospheric modeling discussed in this paper consists of two parts: (1) the tropospheric mapping function to convert the troposphere delay at a certain elevation angle to a zenith delay and (2) an a priori model for the zenith hydrostatic delay (ZHD). Mapping functions and a priori ZHDs derived from numerical weather models (NWMs) provide the best troposphere modeling globally available nowadays. The Vienna Mapping Function 1 (VMF1, Boehm et al. 2006b) and ZHDs derived from the European Centre for Medium-Range Weather Forecasts (ECMWF) NWM are such a sophisticated modeling approach. However, the dependence on external data, the handling of these data, and the assumption that the differences to the Global Mapping Function (GMF) and the Global Pressure and Temperature (GPT) model are small might be

P. Steigenberger (✉)  
Institut für Astronomische und Physikalische Geodäsie,  
Technische Universität München, Arcisstraße 21,  
80333 Munich, Germany  
e-mail: steigenberger@bv.tum.de

J. Boehm  
Institute of Geodesy and Geophysics,  
Vienna University of Technology, Gußhausstraße 27-29,  
1040 Vienna, Austria

V. Tesmer  
Deutsches Geodätisches Forschungsinstitut,  
Alfons-Goppel-Straße 11, 80539 Munich, Germany

*Present Address:*  
V. Tesmer  
OHB-System AG, Universitätsallee 27-29,  
28359 Bremen, Germany

reasons why VMF1 and ECMWF ZHDs are not routinely used in GPS data analysis.

On the other hand, the empirical GMF (Boehm et al. 2006a) and the GPT model (Boehm et al. 2007a) for the computation of the ZHD are easier to use as they do not require external input data. Therefore, this modeling approach is used by most analysis centers of the International GNSS Service (IGS, Dow et al. 2005) nowadays. As GMF and GPT ZHDs or VMF1 and ECMWF ZHDs are usually used together, this paper will focus on the comparison of these modeling options denoted by GMF/GPT and VMF1/ECMWF. However, for some comparisons other combinations of mapping functions and ZHDs will also be used.

Comparisons of different troposphere mapping functions have already been performed by Boehm et al. (2007b), Tesmer et al. (2007) and Vey et al. (2006). Tregoning and Herring (2006) showed that systematic differences between constant ZHDs and GPT-derived ZHDs introduce systematic station height biases of up to 10 mm, in particular in Antarctica. Tesmer et al. (2006) also found systematic height differences when comparing coordinate time series of 49 VLBI telescopes computed with constant a priori delays and a priori delays derived from pressure measurements at the sites. Kouba (2009) already compared the mapping function/a priori ZHD combinations GMF/GPT and VMF1/ECMWF with the precise point positioning (PPP) approach (e.g., Zumberge et al. 1997) at 11 sites and for a time span of 1.5 years. However, because of the larger number of stations and the longer time span used in this study, our results should be more meaningful statistically.

Section 2 describes the tropospheric modeling of geodetic microwave observations and provides more details on the mapping functions and ZHDs mentioned above. The GPS processing resulting in four different global GPS solutions covering all combinations of the two different mapping functions GMF and VMF1 and the two different a priori ZHDs GPT and ECMWF is explained in Sect. 3. The differences of these solutions as regards station coordinates, terrestrial reference frames (TRFs) and station height repeatabilities are shown in Sect. 4. Section 5 discusses the effect of a tropospheric mismodeling (GMF/GPT compared to VMF1/ECMWF) and the implications for atmospheric loading. Tregoning and Herring (2006) already pointed out the destructive interference between ZHD errors and atmospheric loading and Kouba (2009) showed, that this mismodeling partly compensates for atmospheric loading.

## 2 Troposphere modeling

The tropospheric delay is usually separated into a hydrostatic delay that is modeled a priori and a wet delay that is estimated from the space geodetic microwave observations. As

the modeled hydrostatic delays and the estimated wet delays are usually referred to the zenith direction, corresponding mapping functions are required to convert the slant delays in observation direction to the zenith. In addition, troposphere gradients can be estimated to account for asymmetries of the troposphere (e.g., MacMillan 1995; Rothacher et al. 1998).

Most of the recent mapping functions are based on the continued fraction form of Herring (1992). For the VMF1, the coefficients  $a_h$  and  $a_w$  were derived from a rigorous ray-tracing through pressure levels of the ECMWF operational analysis data. These coefficients are provided by TU Vienna<sup>1</sup> as site-specific or global grid ( $2^\circ \times 2.5^\circ$ ) time series with 6-hourly temporal spacing. The coefficients  $b_h$  and  $c_h$  were derived from 1 year of ECMWF data in a least squares fit. Whereas  $b_h$  is constant,  $c_h$  depends on the day of year and the latitude.  $b_w$  and  $c_w$  were taken from the Niell mapping function (Niell 1996) at  $45^\circ$  latitude, since the coefficient  $a_w$  is sufficient to model the dependence of the wet mapping function on latitude (Boehm and Schuh 2004).

The GMF is an empirical mapping function (input arguments are only the day of year and the site location) that is consistent with VMF1. Expressions for the coefficients  $a_h$  and  $a_w$  (mean values and annual signal) were derived from 3 years of ECMWF data and are provided as a spherical harmonic expansion of degree and order 9. The coefficients  $b$  and  $c$  are taken from the VMF1.

Hydrostatic troposphere delays depend primarily on the pressure. GPT provides pressure and temperature based on the location of a station and the day of the year. The hydrostatic part of the Saastamoinen (1973) equation can be used to compute the ZHD from the GPT-derived pressure. Like the GMF, GPT is based on a spherical harmonic expansion (mean values and annual signal) of degree and order 9 derived from 3 years of ECMWF data.

Hydrostatic zenith delays directly derived from numerical integration through pressure level data of NWMs in addition account for short-term as well as inter-seasonal variations. Like the VMF1 coefficients, the ECMWF ZHDs are available on a global  $2^\circ \times 2.5^\circ$  grid with 6 h time resolution. As the ECMWF ZHDs are provided for the heights  $h_M$  of a digital elevation model<sup>2</sup> (DEM) at the grid points, these values have to be extrapolated to the actual station height  $h$ . F. Brunner (2001, personal communication) proposed the extrapolation

$$\text{ZHD}(h) = \text{ZHD}(h_M) - 2.277 \times 10^{-3} \frac{g}{R} \frac{p(h_M)}{T(h_M)} (h - h_M) \quad (1)$$

with  $g$  gravity,  $R$  gas constant,  $p(h_M)$  pressure at height  $h_M$ ,  $T(h_M)$  temperature at height  $h_M$ .  $p(h_M)$  and  $T(h_M)$  can be computed with the GPT model or a standard atmosphere

<sup>1</sup> <http://mars.hg.tuwien.ac.at/~ecmwf1/>.

<sup>2</sup> [http://www.hg.tuwien.ac.at/~ecmwf1/GRID/orography\\_ell](http://www.hg.tuwien.ac.at/~ecmwf1/GRID/orography_ell).

**Table 1** Troposphere mapping functions and hydrostatic a priori delays of the four global GPS solutions discussed in this paper

Solution	Mapping function	Hydrostatic a priori delay
GMF/GPT	GMF	GPT/Saastamoinen
VMF1/GPT	Gridded VMF1	GPT/Saastamoinen
GMF/ECMWF	GMF	Gridded ECMWF ZHDs + extrapolation
VMF1/ECMWF	Gridded VMF1	Gridded ECMWF ZHDs + extrapolation

(e.g., Berg 1948). As will be shown in Sect. 4, this extrapolation is not sufficient for large height differences.

### 3 Global GPS solutions

The global GPS solutions are based on the GPS reprocessing effort of Technische Universität München (TUM), Technische Universität Dresden (TUD) and GeoForschungs-Zentrum (GFZ) Potsdam (Steigenberger et al. 2006). The solutions discussed in this paper were computed with an updated processing scheme, see Steigenberger et al. (2009a). A modified version of the Bernese GPS Software (Dach et al. 2007) was used to process observations from a global network of 202 GPS tracking stations for the time period 1 January 1994 till 31 October 2005. Four solutions covering all combinations of the mapping functions GMF and VMF1 and the hydrostatic a priori delays from GPT and ECMWF have been computed (see Table 1). The grid version of VMF1 was used since for some of the stations of our tracking network the site-specific version of the VMF1 is not available. As the VMF1 coefficients as well the ECMWF ZHDs are provided on  $2^\circ \times 2.5^\circ$  grids with 6-hourly temporal resolution, a spatial bi-linear interpolation and a temporal linear interpolation have been used. For all solutions, an elevation cut-off angle of  $3^\circ$  and an elevation-dependent weighting (weight  $w = \cos^2 z$  with zenith angle  $z$ ) was applied (for the impact of different cut-off angles and elevation-dependent weighting see Tregoning and Herring 2006).

The GPS data are processed in daily batches. The wet troposphere zenith delays are estimated as a continuous piecewise linear function with 2 h parameter spacing. The troposphere gradients in east–west and north–south direction have a parameter spacing of 24 h. The approach for computing a GPS-derived TRF and time series solutions follows Steigenberger et al. (2009b): 1-day normal equations including station positions and pole coordinates have been accumulated. Station coordinates and velocities as well as pole coordinates with daily resolution represented by a continuous piecewise linear function have been estimated in a single program run. The geodetic datum was defined by no-net-rotation conditions for coordinates and velocities of 62 stable IGB00 (Ray et al. 2004) stations. These TRFs have been used for

datum definition in the time series solutions which yielded the final station coordinate time series.

### 4 Comparisons of GMF/GPT and VMF1/ECMWF

The transformation parameters of a 14-parameter similarity transformation between the GMF/GPT TRF and the VMF1/ECMWF TRF are listed in Table 2. A slight shift of 0.7 mm occurs in  $z$ -direction whereas the other translations, the rotation and scale offsets as well as all rates are not significant. The residuals of the 14-parameter similarity transformation (datum stations only) are shown in Fig. 1. The horizontal residuals are all below 0.5 mm (vector length) with a mean value of 0.25 mm. They show a systematic pattern pointing to a virtual point located in the southern Indian ocean. Although the reason for this effect is not clear, Tesmer et al. (2007) reported a similar behavior for VLBI solutions computed with different mapping functions. However, one has to be aware of the small magnitude of the horizontal residuals.

As expected, the height residuals are larger and range from  $-5.9$  mm for Davis (Antarctica) to  $+6.4$  mm for Mauna Kea (Hawaii). However, the absolute value of the height residuals is below 1 mm for 81% of the stations and below 0.5 mm for 58% of the stations. These results are in general accordance with the VLBI-based GMF/VMF1 comparisons of Tesmer et al. (2007). In contrast to the horizontal residuals, the vertical residuals do not show a clear systematic pattern although some larger negative residuals are present in Antarctica. Some of the larger height residuals are related to extrapolation errors of Eq. 1 as well as the height extrapolation of GPT. For example, Mauna Kea has an ellipsoidal station height of 3,755 m whereas the interpolated height of the ECMWF DEM is 322 m. This extrapolation for a height difference of more than 3 km is probably the main reason for the height residual of  $+6.4$  mm. The horizontal velocity residuals are negligible (a few hundredth of a millimeter per year). The vertical velocity residuals are in general below 0.2 mm/year with an absolute mean value of 0.08 mm/year.

Mean station height repeatabilities (average of all stations) of the four different troposphere modeling approaches are listed in Table 3. The first column contains repeatabilities computed as WRMS values of the differences between the daily solutions and the TRF solution, i.e., all

**Table 2** Transformation parameters of a 14-parameter similarity transformation between GMF/GPT and VMF1/ECMWF terrestrial reference frames

	Offset	Rate
Translation <i>X</i>	0.18 ± 0.08 (mm)	0.02 ± 0.08 (mm/year)
Translation <i>Y</i>	-0.07 ± 0.08 (mm)	0.02 ± 0.08 (mm/year)
Translation <i>Z</i>	0.71 ± 0.08 (mm)	-0.02 ± 0.08 (mm/year)
Rotation <i>X</i>	0.01 ± 0.01 (mas)	0.00 ± 0.01 (mas/year)
Rotation <i>Y</i>	0.00 ± 0.01 (mas)	0.00 ± 0.01 (mas/year)
Rotation <i>Z</i>	0.00 ± 0.01 (mas)	0.00 ± 0.01 (mas/year)
Scale	-0.03 ± 0.01 (ppb)	0.00 ± 0.01 (ppb/year)

**Fig. 1** Residuals of a 14-parameter similarity transformation between GMF/GPT and VMF1/ECMWF terrestrial reference frames. The arrows refer to the horizontal, the color scale to the height residuals

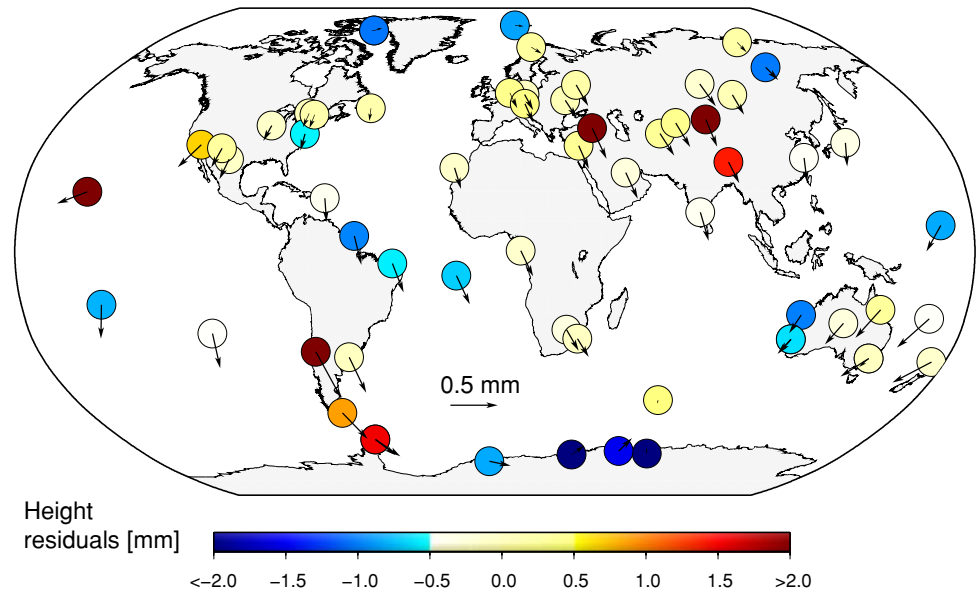


**Table 3** Mean station height repeatabilities: *TRF* stands the repeatabilities from the reference frame solution; *Weekly 2004* for the repeatabilities of seven daily solutions w.r.t. a weekly solution, averaged for the year 2004

Solution	TRF (mm)	Weekly 2004 (mm)
GMF/GPT	9.30	5.35
GMF/ECMWF	9.41	5.46
VMF1/GPT	9.12	5.15
VMF1/ECMWF	9.38	5.28

systematic and random signals differing from the linear TRF model contribute to these values. The second column represents a mean value of repeatabilities from weekly solutions for the year 2004, i.e., the deviations of seven daily solution w.r.t. the combined weekly solution. If one compares solutions with the same a priori ZHD (GMF/GPT vs. VMF1/GPT or GMF/ECMWF vs. VMF1/ECMWF) one can see that VMF1 performs slightly better than GMF. This result is consistent with the VLBI-derived repeatabilities of [Tesmer et al. \(2007\)](#). On the other hand, a comparison of solutions

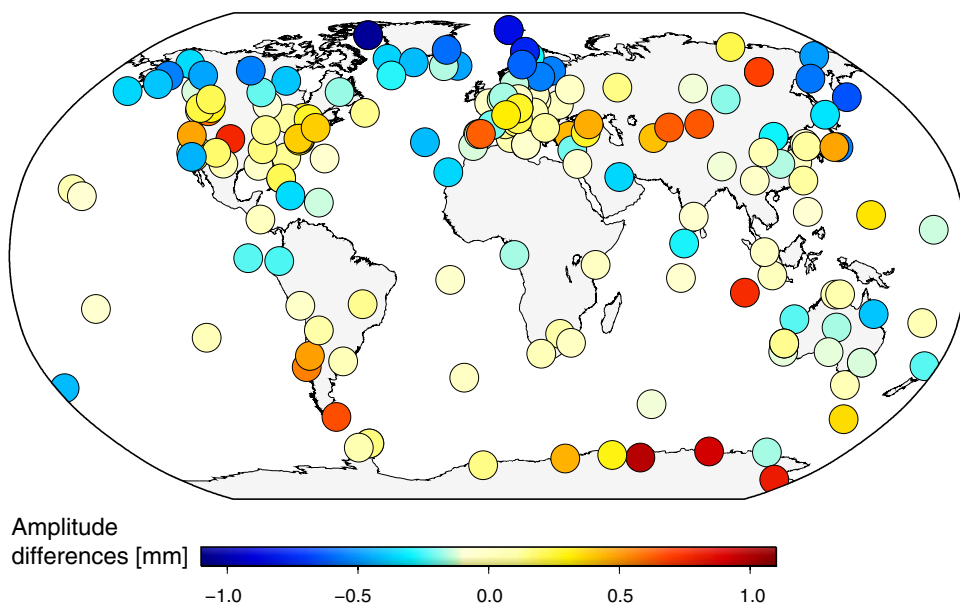
with the same mapping function (GMF/GPT vs. GMF/ECMWF or VMF1/GPT vs. VMF1/ECMWF) shows that GPT results in better repeatabilities than ECMWF ZHDs for both the TRF and the weekly repeatabilities. As will be shown in Sect. 5, this effect is related to the partial compensation of atmospheric loading by applying the GPT model.

Another result from these comparisons is that the amplitudes of annual signals in the station height are affected by different troposphere modeling. The amplitude differences between the solutions, GMF/GPT minus VMF1/ECMWF, are shown in Fig. 2. They range from -1.1 to +1.0 mm with an absolute mean value of 0.3 mm and a slight latitude dependence. In Antarctica, the VMF1/ECMWF station height amplitudes are in general smaller, whereas the situation in the high northern latitude is the opposite.

### 5 Implications for atmospheric loading

The differences between the hydrostatic and the wet mapping functions result in a height error if an erroneous a priori ZHD is applied: the difference between the true and the

**Fig. 2** Amplitude differences between annual signals determined from GMF/GPT and VMF1/ECMWF station height time series



erroneous ZHD is mapped with the wet instead of the hydrostatic mapping function (or vice versa), thus biasing the estimated troposphere delays as well as station heights. Although GPT was generated from ECMWF data (i.e., there are almost no systematic mean biases between GPT and ECMWF ZHDs), there are small but systematic time-dependent differences between the ZHDs of both models as GPT only considers temporal pressure variations with a simple annual sine model. Furthermore, a spatial smoothing is introduced as GPT is a spherical harmonic expansion of degree and order 9 whereas the ECMWF ZHD grids have a resolution of degree and order of about 80 at the equator. However, [Boehm et al. \(2008\)](#) showed that the agreement between GPT and the ECMWF grids is not too bad.

As a simple approximation, the ZHD is directly related to the pressure  $p$  by

$$\text{ZHD} \approx 0.00227768 \frac{\text{m}}{\text{mbar}} \cdot p \tag{2}$$

and the station height changes,  $\Delta H_{\text{AL}}$ , due to atmospheric loading are proportional to the negative of the difference between the pressure and a reference pressure:

$$\Delta H_{\text{AL}} \approx -k(p - p_{\text{ref}}) \tag{3}$$

with  $k$  atmospheric loading regression coefficient (m/mbar),  $p_{\text{ref}}$  reference pressure. These relationships are responsible for the partial compensation of atmospheric loading by mismodeling the ZHDs as the zenith delays and the height estimates are negatively correlated due to the erroneous mapping. An example for this effect has already been shown by [Tregoning and Herring \(2006\)](#).

Figure 3 explains this effect for an ideal case. It is assumed that there are no other error sources than the ZHD and that the atmospheric loading signal is the only signal affecting

the station height. If the periodic true ZHD (blue line) is introduced, the atmospheric loading signal can completely be recovered and the resulting height estimates are equal to this loading signal, see Fig. 3a.

If an erroneous ZHD is applied (for simplicity a constant ZHD, dashed green line in Fig. 3b, top), the differences between the true and the erroneous ZHD (represented by arrows) result in changes in the estimated station height. As ZHD and atmospheric loading are anti-correlated (see Eqs. 2, 3), the height estimates have a smaller amplitude (solid green line in Fig. 3b, bottom) than the atmospheric loading signal. Therefore, the mismodeling of the a priori ZHDs results in a partial compensation of the atmospheric loading. As the differences between GPT and the ECMWF delays are much smaller than the differences between a sinusoidal and a constant ZHD, the real effect is of course smaller for the GPT model than in the scenario discussed above.

As an example based on real data, Fig. 4a shows the GPT and ECMWF ZHDs for Wuhan, China. Although the GPT-derived ZHDs represent in general a simplified mean behavior of the ECMWF delays, there are systematic differences due to the spatial and temporal smoothing of GPT, see Fig. 4b. In particular in wintertime larger discrepancies occur: the ECMWF ZHDs are on average about 1 cm larger than the GPT-derived ZHDs. The differences between the estimated station heights, in sense VMF1/ECMWF minus VMF1/GPT, are shown in Fig. 4c. Figure 4d shows the atmospheric loading corrections from [Petrov and Boy \(2004\)](#).<sup>3</sup> These atmospheric loading corrections were derived from a different weather model than ECMWF, namely the National Centers for Environmental Prediction (NCEP)

<sup>3</sup> <http://gemini.gsfc.nasa.gov/aplo/>.

**Fig. 3** Impact of tropospheric mismodeling on estimated station heights: **a** ideal case, the complete atmospheric loading signal is recovered by the height estimates. **b** Erroneous (constant) ZHD (dashed green line), a part of the atmospheric loading signal is compensated by the mismodeling of the hydrostatic a priori delay

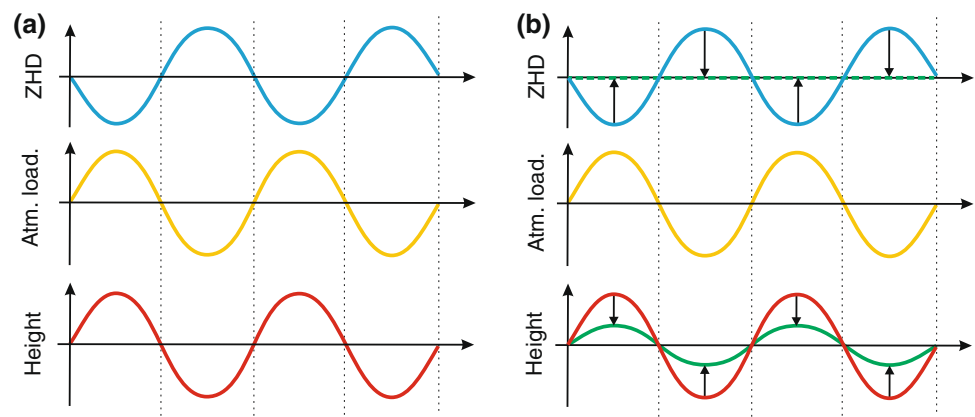
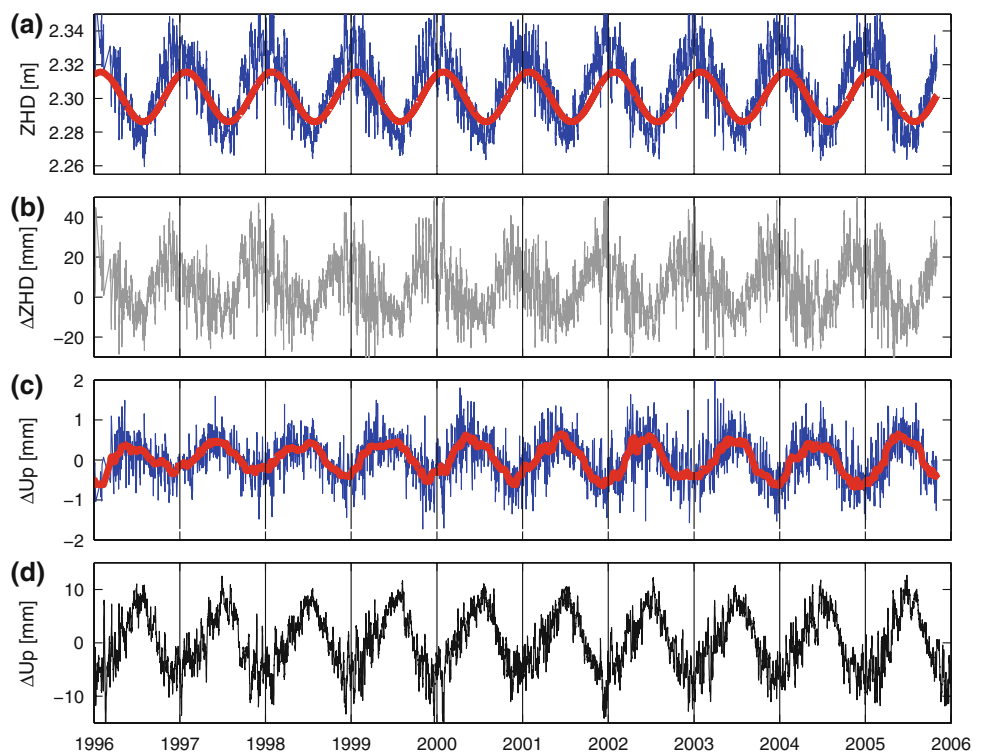


**Fig. 4** Time series for Wuhan: **a** hydrostatic a priori delays from GPT (red) and ECMWF (blue). **b** ZHD differences ECMWF – GPT. **c** Station height differences, VMF1/ECMWF – VMF1/GPT; the red line indicates a 50-day median. **d** Atmospheric loading corrections provided by Petrov and Boy (2004)



model. However, the surface pressure differences between NCEP and ECMWF are rather small and are not expected to influence the results significantly. A clear annual signal can be seen in both time series, the station height differences and the atmospheric loading corrections. Although the order of magnitude of the station height differences is much smaller than those of the atmospheric loading corrections, it is evident that both signals show a good agreement in phase. Therefore, the GPT-derived ZHDs partly compensate for the atmospheric loading effect.

The homogeneously reprocessed GPS time series of station heights provides an ideal basis to study the impact of different troposphere modeling and atmospheric loading corrections in more detail. All stations with time series longer than 2 years have been considered. After removing stations

with frequent or large data gaps or with known problems, 183 out of 202 stations remain. To simplify matters, the atmospheric loading corrections have been applied a posteriori by taking the correction at 12:00 UT. The mean station height repeatabilities with and without atmospheric loading corrections are shown in Fig. 5. The results without atmospheric loading corrections are consistent with the repeatabilities in Table 3 already discussed above: VMF1 performs better than GMF and for both mapping functions, the ECMWF a priori ZHDs result in worse repeatabilities compared to GPT. However, after correcting for atmospheric loading, the repeatabilities of the solutions with ECMWF ZHDs are slightly better for both GMF and VMF1. Although the differences are on the level of a few tenths of a millimeter, Fig. 5 confirms the theoretical considerations discussed above.

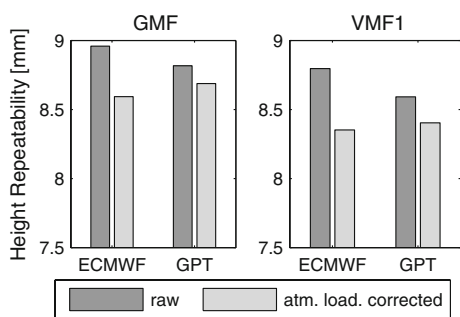


**Fig. 5** Station height repeatabilities without (*raw*) and with atmospheric loading corrections

However, for stations near the coast the largest part of the atmospheric loading is absorbed by the inverted barometer effect of the ocean. This fact is confirmed by Fig. 6 which shows the repeatability differences of solution VMF1/ECMWF with and without atmospheric loading corrections. Pronounced repeatability improvements occur only in the northern central part of North America, in Europe, and in the central part of Asia. The coastal sites in general show a repeatability difference below 0.5 mm. Therefore, a separate statistics for stations at least 200 km away from the coast is included in Table 4. For this subset of stations, the repeatability improvement when correcting for atmospheric loading is about a factor of two larger compared to all stations.

The results discussed above are in general agreement with Kouba (2009) who compared GMF/GPT and VMF1/ECMWF by PPP solutions of 11 stations covering a time period of 1.5 years. In addition to Table 6 of Kouba (2009), J. Kouba (2008, personal communication) provided an updated solution including VMF1/GPT repeatabilities (see Table 4). Some important differences between the analysis

of Kouba (2009) and those presented here should be emphasized:

- PPP solutions versus global network solution
- 1.5 versus 11.8 years
- 11 versus 183 stations
- atmospheric loading regression coefficients versus corrections from Petrov and Boy (2004).

As the time period as well as the number of stations is much larger compared to J. Kouba (2008, personal communication), the results presented in this paper are assumed to be more reliable as the impact of outliers is smaller and more areas of the world are covered. First of all, all of our network solutions provide better height repeatabilities compared to the corresponding PPP solutions of J. Kouba (2008, personal communication). The repeatability improvement when correcting for atmospheric loading is larger when using the corrections from Petrov and Boy (2004) compared to the simple regression coefficient approach. The largest repeatability improvement [consistently for our solution and the J. Kouba (2008, personal communication) solution] can be achieved for solution VMF1/ECMWF: VMF1 is the more precise mapping function compared to GMF and only the ECMWF ZHDs are able to reveal the full loading signal. The partial compensation of atmospheric loading by the GPT-derived ZHDs resulting in better repeatabilities for the raw time series is visible for our as well as for the J. Kouba (2008, personal communication) solutions.

Although GMF provides a worse height repeatability compared to VMF1, the raw GMF/GPT repeatabilities of J. Kouba (2008, personal communication) are 0.2 mm smaller than the corresponding VMF1/ECMWF repeatabilities,

**Fig. 6** Repeatability differences for solution VMF1/ECMWF with and without atmospheric loading corrections

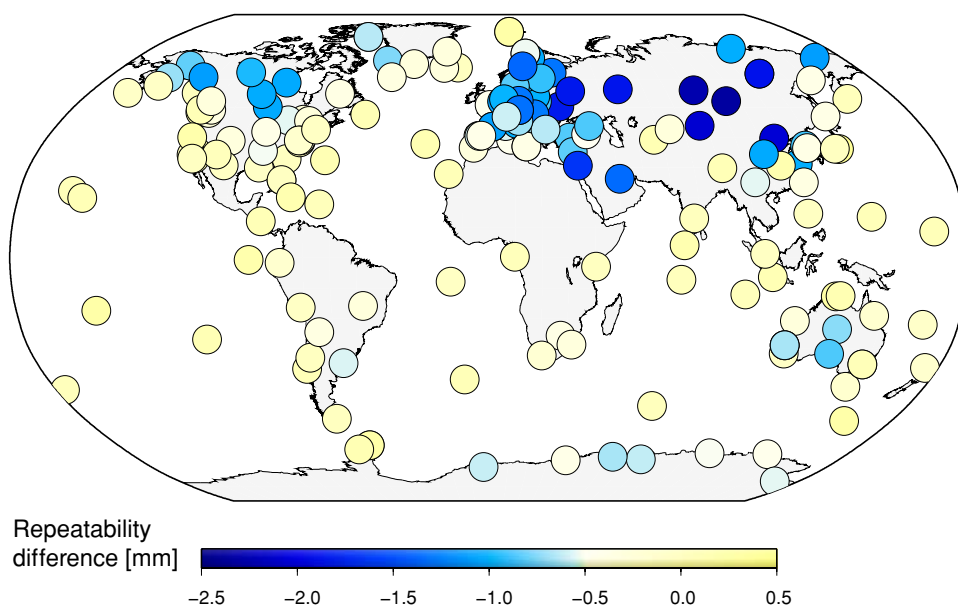


**Table 4** Station height repeatabilities without (*raw*) and with atmospheric loading corrections (*alcor*)

Solution	This paper all			This paper >200 km			J. Kouba (2008, personal communication)		
	Raw (mm)	Alcor (mm)	Red (%)	Raw (mm)	Alcor (mm)	Red (%)	Raw (mm)	Alcor (mm)	Red (%)
GMF/GPT	8.81	8.69	1.4	8.73	8.35	4.4	10.03	9.90	1.3
GMF/ECMWF	8.96	8.59	4.1	8.94	8.25	7.7	–	–	–
VMF1/GPT	8.59	8.40	2.2	8.49	8.11	4.5	10.00	9.78	2.2
VMF1/ECMWF	8.80	8.35	5.1	8.73	8.02	8.1	10.23	9.87	3.5

The repeatability reduction when correcting for atmospheric loading is given in the columns *Red*. For the columns *This paper >200 km*, only stations with a distance of more than 200 km to the nearest coast have been considered

whereas the repeatabilities of our raw GMF/GPT and VMF1/ECMWF solutions are on the same level, which can be attributed to the different number of stations used for the statistics (11 vs. 183). The slightly better performance of the VMF1/GPT PPP solutions compared to the VMF1/ECMWF PPP solutions after correcting for atmospheric loading was not expected and might also be related to the small number of only 11 stations. As GPT already compensates for some part of the atmospheric loading effect, the repeatabilities of the solutions with GPT-derived ZHDs are expected to have a worse repeatability compared to the ECMWF ZHDs if atmospheric loading is corrected for. This is indeed the case for our VMF1/ECMWF solution.

## 6 Conclusions

The analyses presented in this paper have shown that VMF1 provides slightly better station height repeatabilities than GMF. On the other hand, the long-term station position differences are in general small: they are on the sub-millimeter level for the horizontal component and in general within  $\pm 1$  mm for the station heights. Due to the partial compensation of atmospheric loading by mismodeling the a priori ZHDs, GPT-derived ZHDs result in a better station height repeatability compared to ECMWF ZHDs if atmospheric loading is not corrected for. On the other hand, the application of ZHDs derived from numerical weather models is essential if the coordinate time series should be used to reveal atmospheric loading signals.

An open issue is why the repeatability improvements are so small when correcting for atmospheric loading (only 5% for all stations and 8% for inland stations of solution VMF1/ECMWF). Possible explanations are other systematic effects in the GPS-derived station height time series or weaknesses in the computation of the atmospheric loading corrections. However, the small repeatability improvement is in good agreement with Tesmer et al. (2006) who found an improvement of 4% when comparing VLBI solutions with and without atmospheric loading corrections. Tesmer et al.

(2008) showed that large discrepancies between the loading corrections of Petrov and Boy (2004) and ECMWF pressure values multiplied with VLBI-derived atmospheric loading coefficients are present for several stations. These studies indicate that there might be some deficiencies of the atmospheric loading corrections that should be studied in more detail in the future.

**Acknowledgments** The authors would like to thank the International GNSS Service (Dow et al. 2005) for providing global GPS observation data.

## References

- Berg H (1948) Allgemeine Meteorologie. Dümmlers Verlag, Bonn
- Boehm J, Schuh H (2004) Vienna mapping functions in VLBI analyses. *Geophys Res Lett* 31:L01603. doi:10.1029/2003GL018984
- Boehm J, Niell A, Tregoning P, Schuh H (2006a) Global Mapping Function (GMF): a new empirical mapping function based on numerical weather model data. *Geophys Res Lett* 33:L07304. doi:10.1029/2005GL025546
- Boehm J, Werl B, Schuh H (2006b) Troposphere mapping functions for GPS and very long baseline interferometry from European Centre for Medium-Range Weather Forecasts operational analysis data. *J Geophys Res* 111:B02406. doi:10.1029/2005JB003629
- Boehm J, Heinkelmann R, Schuh H (2007a) Short note: a global model of pressure and temperature for geodetic applications. *J Geod* 81(10):679–683. doi:10.1007/s00190-007-0135-3
- Boehm J, Mendes Cerveira PJ, Schuh H, Tregoning P (2007b) The impact of tropospheric mapping functions based on numerical weather models on the determination of geodetic parameters. In: Tregoning P, Rizos C (eds) *Dynamic planet—monitoring and understanding a dynamic planet with geodetic and oceanographic tools*. Springer, International Association of Geodesy Symposia, vol 130, pp 837–843. doi:10.1007/978-3-540-49350-1\_118
- Boehm J, Schuh H, Mendes Cerveira PJ, Heinkelmann R (2008) Reference pressure for the Global Geodetic Observing System GGOS. IVS memorandum 2008-002v01. <ftp://ivscc.gsfc.nasa.gov/pub/memos/ivs-2008-002v01.pdf>
- Dach R, Hugentobler U, Fridez P, Meindl M (eds) (2007) *Bernese GPS software version 5.0*. Astronomical Institute, University of Bern, Bern
- Dow J, Neilan R, Gendt G (2005) The International GPS Service: celebrating the 10th anniversary and looking to the next decade. *Adv Space Res* 36(3):320–326. doi:10.1016/j.asr.2005.05.125

- Herring T (1992) Modeling atmospheric delays in the analysis of space geodetic data. In: de Munck J, Spoelstra T (eds) *Publications on geodesy (New Series)*, Netherlands Geodetic Commission, Delft, vol 36, pp 157–164, ISBN: 90 6132 243 X
- Kouba J (2009) Testing of Global Pressure/Temperature (GPT) Model and Global Mapping Function (GMF) in GPS analyses. *J Geod* 83(3–4):199–208. doi:[10.1007/s00190-008-0229-6](https://doi.org/10.1007/s00190-008-0229-6)
- MacMillan DS (1995) Atmospheric gradients from very long baseline interferometry observations. *Geophys Res Lett* 22(9):1041–1044
- Niell A (1996) Global mapping functions for the atmosphere delay at radio wavelengths. *J Geophys Res* 101(B2):3227–3246. doi:[10.1029/95JB03048](https://doi.org/10.1029/95JB03048)
- Petrov L, Boy JP (2004) Study of the atmospheric pressure loading signal in very long baseline interferometry observations. *J Geophys Res* 109:B03405. doi:[10.1029/2003JB002500](https://doi.org/10.1029/2003JB002500)
- Ray J, Dong D, Altamimi Z (2004) IGS reference frames: status and future improvements. *GPS Solut* 8(4):251–266. doi:[10.1007/s10291-004-0110-x](https://doi.org/10.1007/s10291-004-0110-x)
- Rothacher M (2002) Estimation of station heights with GPS. In: Drewes H, Dodson A, Fortes L, Sanchez L, Sandoval P (eds) *Vertical reference systems*. Springer, International Association of Geodesy Symposia, vol 124, pp 81–90, ISBN: 3-540-43011-3
- Rothacher M, Springer T, Schaer S, Beutler G (1998) Processing strategies for regional GPS networks. In: Brunner F (ed) *Advances in positioning and reference frames*. Springer, International Association of Geodesy Symposia, vol 118, pp 93–100, ISBN: 3-540-64604-3
- Saastamoinen J (1973) Contributions to the theory of atmospheric refraction. *Bull Geod* 107:13–34. doi:[10.1007/BF02522083](https://doi.org/10.1007/BF02522083)
- Snajdrova K, Boehm J, Willis P, Haas R, Schuh H (2005) Multi-technique comparison of tropospheric zenith delays derived during the CONT02 campaign. *J Geod* 79(10–11):613–623. doi:[10.1007/s00190-005-0010-z](https://doi.org/10.1007/s00190-005-0010-z)
- Steigenberger P, Rothacher M, Dietrich R, Fritsche M, Rülke A, Vey S (2006) Reprocessing of a global GPS network. *J Geophys Res* 111:B05402. doi:[10.1029/2005JB003747](https://doi.org/10.1029/2005JB003747)
- Steigenberger P, Tesmer V, Krügel M, Thaller D, Schmid R, Vey S, Rothacher M (2007) Comparisons of homogeneously reprocessed GPS and VLBI long time-series of troposphere zenith delays and gradients. *J Geod* 81(6–8):503–514. doi:[10.1007/s00190-006-0124-y](https://doi.org/10.1007/s00190-006-0124-y)
- Steigenberger P, Rothacher M, Fritsche M, Rülke A, Dietrich R (2009a) Quality of reprocessed GPS satellite orbits. *J Geod* 83(3–4):241–248. doi:[10.1007/s00190-008-0228-7](https://doi.org/10.1007/s00190-008-0228-7)
- Steigenberger P, Tesmer V, Schmid R, Rothacher M, Rülke A, Fritsche M, Dietrich R (2009b) Effects of different antenna phase center models on GPS-derived reference frame. In: Drewes H (ed) *GRF2006—geodetic reference frames*. Springer (accepted)
- Tesmer V, Boehm J, Heinkelmann R, Schuh H (2006) Impact of analysis options on the TRF, CRF and position time series estimated from VLBI. In: Behrend D, Baver K (eds) *International VLBI service for geodesy and astrometry 2006 general meeting proceedings, NASA/CP-2006-214140*, NASA, Greenbelt, pp 243–251
- Tesmer V, Boehm J, Heinkelmann R, Schuh H (2007) Effect of different tropospheric mapping functions on the TRF, CRF and position time-series estimated from VLBI. *J Geod* 81(6–8):409–421. doi:[10.1007/s00190-006-0126-9](https://doi.org/10.1007/s00190-006-0126-9)
- Tesmer V, Boehm J, Meisel B, Rothacher M, Steigenberger P (2008) Atmospheric loading coefficients determined from homogeneously reprocessed GPS and VLBI height time series. In: Finkelstein A, Behrend D (eds) *Measuring the future*, proceedings of the fifth IVS general meeting, pp 307–313
- Tregoning P, Herring TA (2006) Impact of a priori zenith hydrostatic delay errors on GPS estimates of station heights and zenith total delays. *Geophys Res Lett* 33(L23303). doi:[10.1029/2006GL027706](https://doi.org/10.1029/2006GL027706)
- Vey S, Dietrich R, Fritsche M, Rülke A, Rothacher M, Steigenberger P (2006) Influence of mapping function parameters on global GPS network analyses: comparisons between NMF and IMF. *Geophys Res Lett* 33:L01814. doi:[10.1029/2005GL024361](https://doi.org/10.1029/2005GL024361)
- Zumberge JF, Heflin MB, Jefferson DC, Watkins MM, Webb FH (1997) Precise point positioning for the efficient and robust analysis of GPS data from large networks. *J Geophys Res* 102(B3):5005–5017. doi:[10.1029/96JB03860](https://doi.org/10.1029/96JB03860)